

Supplementary material

In vitro anti-leishmanial effect of metallic meso-substituted porphyrin derivatives against Leishmania braziliensis and Leishmania panamensis promastigotes properties

Synthesis

5,10,15,20-tetrakis(4-ethylphenyl)porphyrin-Zn(II) (**2**): A mixture of **(1)** (0.2755 mmol) and ZnCl₂ (1.4673 mmol) in DMF (20 mL) was stirring by 4 hours at room temperature. The reaction mixture was cooled in ice-water bath; the formed precipitate was filtered and dried at ambient temperature; **(2)** was purified through column chromatography with silica gel (2.5 x 24 cm), petroleum ether:ethyl acetate (PE:EA) was using as mobile phase 3:1 (rf = 0.87). Yield: 0.150 g, 75 %; melting point > 300 °C; UV-Vis (ethyl acetate) λ (nm): 422, 556, 597; FT-IR-ATR (cm⁻¹): C_{sp3}-H (2960.44), C=C (1650.32), C=N (992.39), C-N (851.54); Anal. Elem. Calc. for C₅₂H₄₄N₄Zn (%): C (79.05), H (5.61), N (7.10), Zn (8.27); Anal. Elem. Found C₅₂H₄₄N₄Zn (%): (79.02), H (5.60), N (7.09), Zn (8.28).

5,10,15,20-tetrakis(4-ethylphenyl)porphyrin-Sn(IV) (**3**): A mixture of **(1)** (0.2755 mmol) and SnCl₂.2H₂O (0.8865 mmol) in DMF (20 mL) was stirring by 6 hours at room temperature. The reaction mixture was cooled in ice-water bath; the formed precipitate was filtered and dried at ambient temperature; **(3)** was purified through column chromatography with silica gel, PE:EA was used as mobile phase 3:1 (rf = 0.80). Yield: 0.120 g, 60 %; melting point > 300 °C; UV-Vis (ethyl acetate) λ (nm): 415, 514, 549; FT-IR-ATR (cm⁻¹): C_{sp3}-H (2960.44), C=C (1470.55), C=N (956.25), C-N (846.32); Anal. Elem. Calc. for C₅₂H₄₄N₄Cl₂Sn (%): C (68.29), H (4.84), N (6.13), Cl(7.75), Sn (12.97).

5,10,15,20-tetrakis(4-ethylphenyl)porphyrin-Mn(II) (**4**): A mixture of **(1)** (0.2755 mmol) and MnCl₂.4H₂O (1.0105 mmol) in DMF (20 mL) was stirring by 6 hours at room temperature. The reaction mixture was cooled in ice-water bath; the formed precipitate was filtered and dried at ambient temperature; **(4)** was purified through column chromatography with silica gel, PE:EA was used as mobile phase 2:1 (rf = 0.89). Yield: 0.118 g, 59 %; melting point > 300 °C; UV-Vis (ethyl acetate) λ (nm): 416, 469, 549; FT-IR-ATR (cm⁻¹): C_{sp3}-H (2960.44), C=C (1181.04), C=N (964.71), C-N

(846.18); Anal. Elem. Calc. for $C_{52}H_{44}N_4Mn$ (%): C (80.11), H (5.65), N (7.19), Mn (7.05). Anal. Elem. Found. for $C_{52}H_{44}N_4Mn$ (%): C (80.08), H (5.69), N (7.18), Mn (7.04).

5,10,15,20-tetrakis(4-ethylphenyl)porphyrin-Ni(II) (**5**): A mixture of (**1**) (0.2755 mmol) and $NiCl_2 \cdot 6H_2O$ (0.8414 mmol) in DMF (20 mL) was stirring by 6 hours at room temperature. The reaction mixture was cooled in ice-water bath; the formed precipitate was filtered and dried at ambient temperature; (**5**) was purified through column chromatography with silica gel, PE:EA was used as mobile phase 3:1 (rf = 0.69). Yield: 0.121 g, 60.5 %; melting point > 300 °C; UV-Vis ethyl acetate λ (nm): 418, 592; FT-IR-ATR (cm^{-1}): C_{sp^3-H} (2960.44), C=C (1454.55), C=N (1002.06), C-N (818.64); Anal. Elem. Calc. for $C_{52}H_{44}N_4Ni$ (%): C (79.72), H (5.62), N (7.16), Ni (7.50). Anal. Elem. Found. for $C_{52}H_{44}N_4Ni$, (%): C (79.70), H (5.66), N (7.15), Ni (7.49).

5,10,15,20-tetrakis(4-ethylphenyl)porphyrin-Al(III) (**6**): A mixture of (**1**) (0.2755 mmol) and $AlCl_3$ (1.4999 mmol) in DMF (30 mL) was stirring by 8 hours at room temperature. The reaction mixture was cooled in ice-water bath; the formed precipitate was filtered and dried at ambient temperature; (**6**) was purified through column chromatography with silica gel, PE:EA was used as mobile phase 3:1 (rf = 0.79). Yield: 0.141 g, 70.5 %; melting point > 300 °C; UV-Vis (ethyl acetate) λ (nm): 416, 513, 645; FT-IR-ATR (cm^{-1}): C_{sp^3-H} (2967.96), C=C (1601.84), C=N (1183.38), C-N (826.31); Anal. Elem. Calc. for $C_{52}H_{44}N_4AlCl$ (%): C (79.34), H (5.60), N (7.12), Al (3.43), Cl (5.51). Anal. Elem. Calc. for $C_{52}H_{44}N_4AlCl$ (%): C (79.32), H (5.63), N (7.12), Al (3.43), Cl (5.50).

5,10,15,20-tetrakis(4-ethylphenyl)porphyrin-V(III) (**7**): A mixture (**1**) (0.2755 mmol) and VCl_3 (1.2714 mmol) in DMF (30 mL) was stirring by 8 hours at 100 °C. The reaction mixture was cooled in ice-water bath; the formed precipitate was filtered and dried at ambient temperature; (**7**) was purified through column chromatography with silica gel, PE:EA was used as mobile phase 1:3 (rf = 0.79). Yield: 0.138 g, 69 %; melting point > 300 °C; UV-Vis (ethyl acetate) λ (nm): 415, 515, 550, 594; FT-IR-ATR (cm^{-1}): C_{sp^3-H} (2959.83), C=C (1603.72), C=N (1184.93), C-N (824.22); Anal. Elem. Calc. for $C_{52}H_{44}N_4VCl$ (%): C (77.0), H (5.43), N (6.91), V (6.29), Cl (4.37). Anal. Elem. Calc. for $C_{52}H_{44}N_4VCl$ (%): C (76.98), H (5.47), N (6.90), V (6.28), Cl (4.37).

Characterization

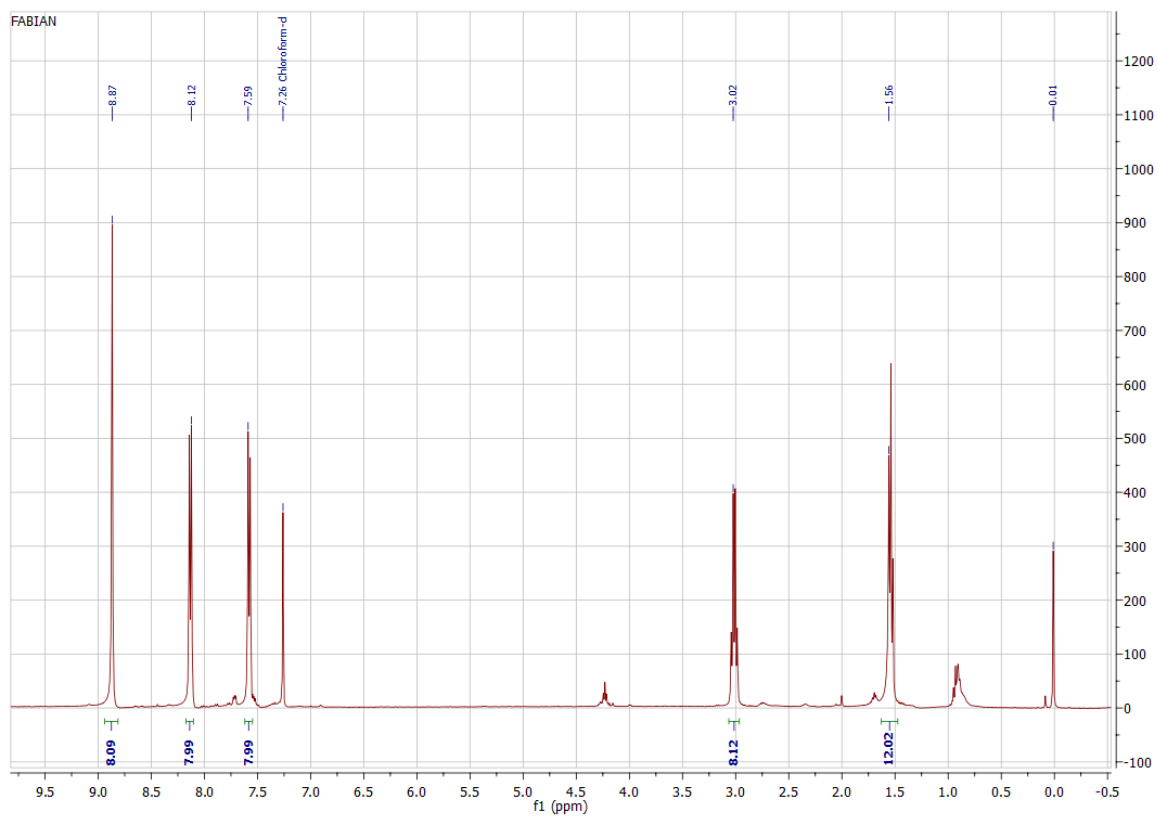


Figure S1. ^1H RMN of (1, Ph).

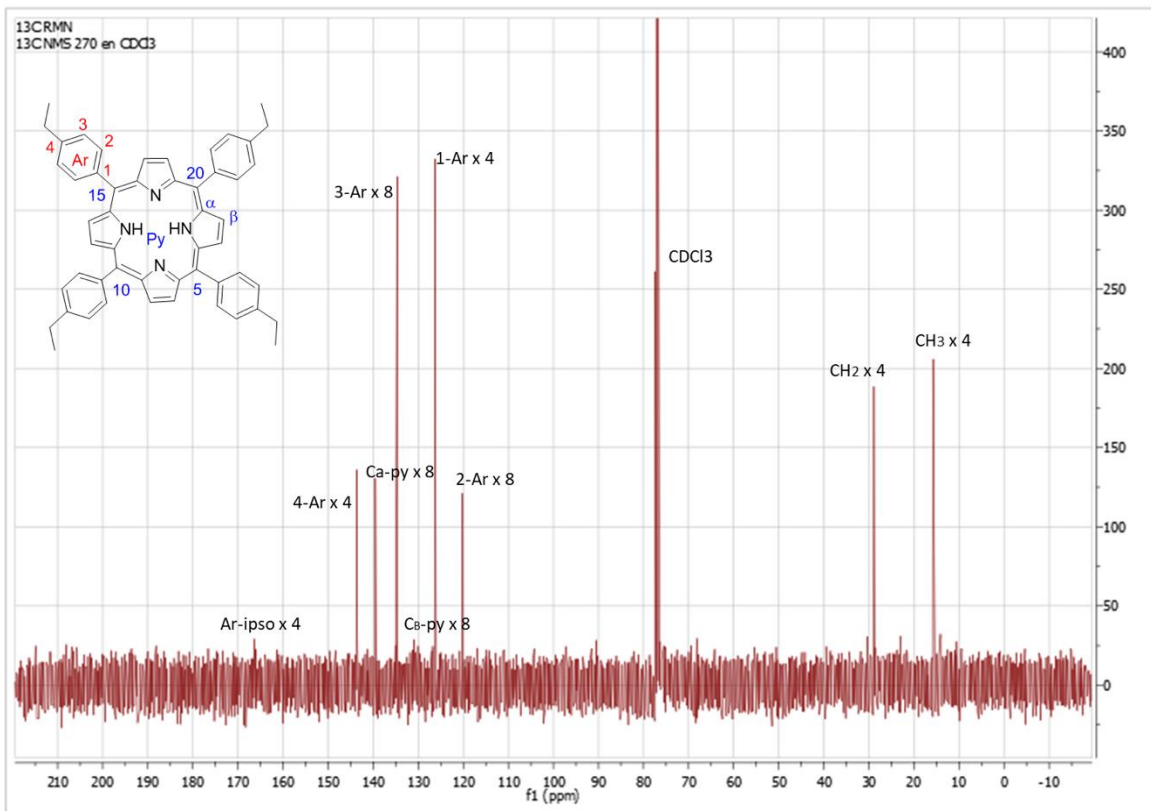


Figure S2. ¹³C RMN of (1, Ph).

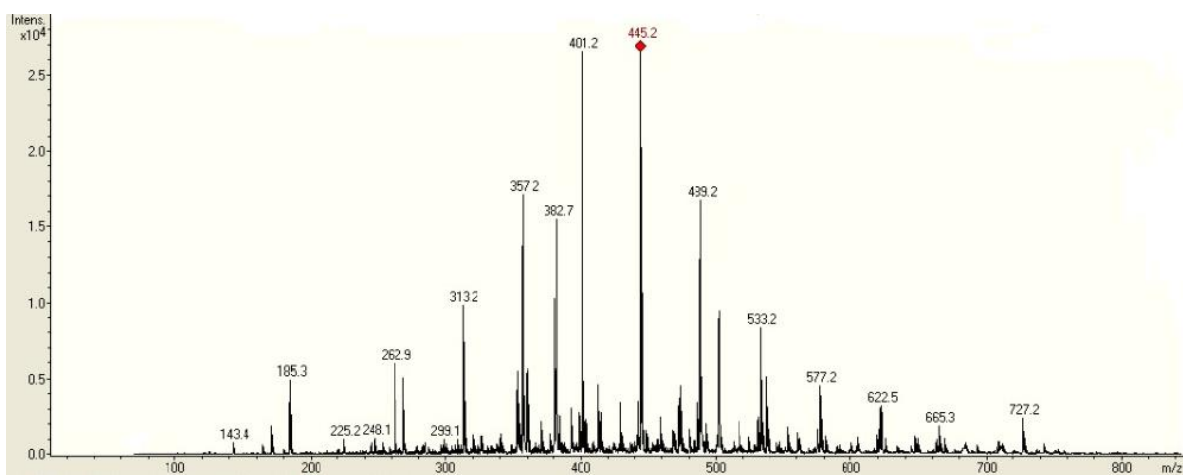


Figure S3. Electrospray ionization tandem mass spectrum of (1, Ph).

FTIR spectra

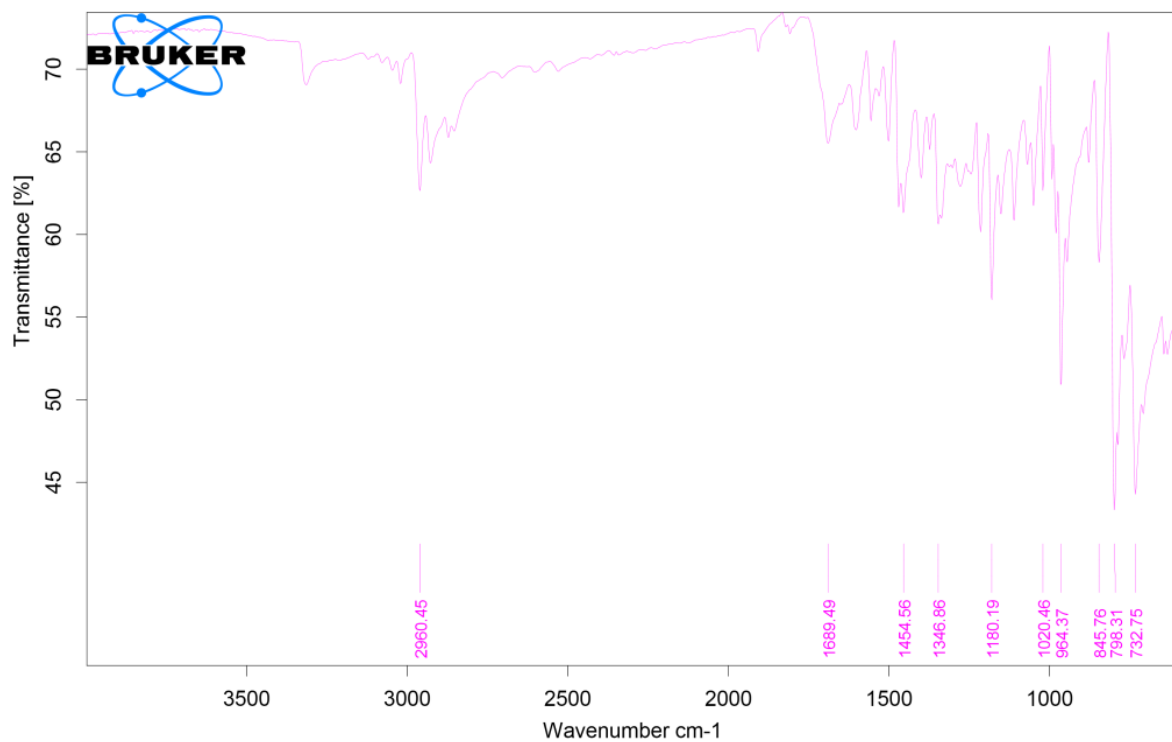


Figure S4. FTIR spectrum of (1, Ph).

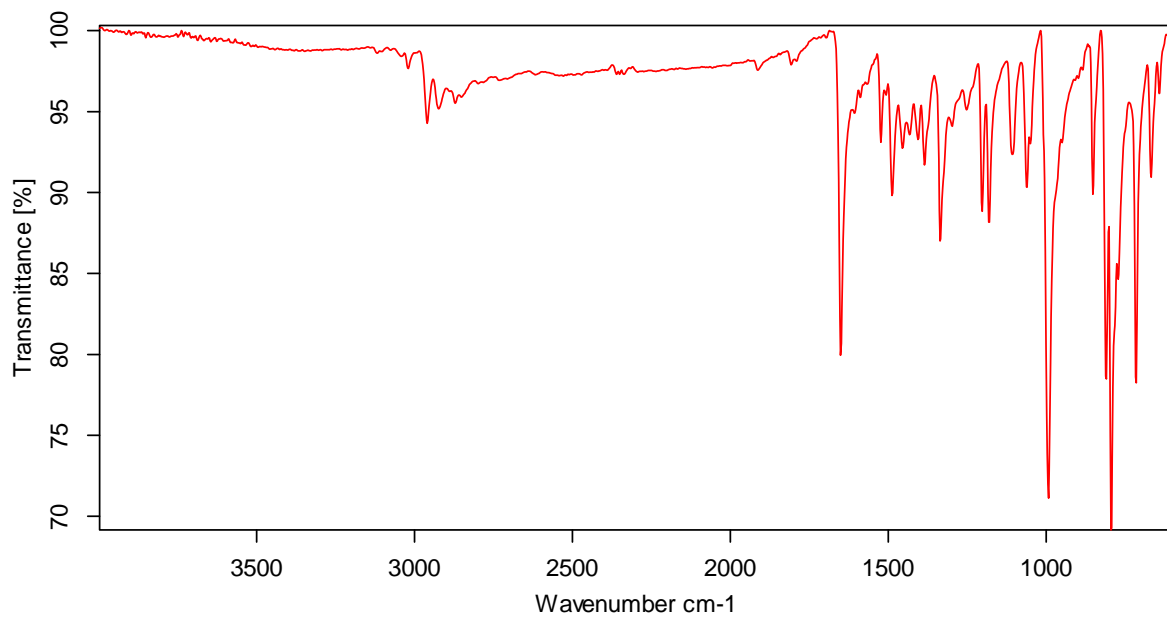


Figure S5. FTIR spectrum of (2, Ph-Zn).

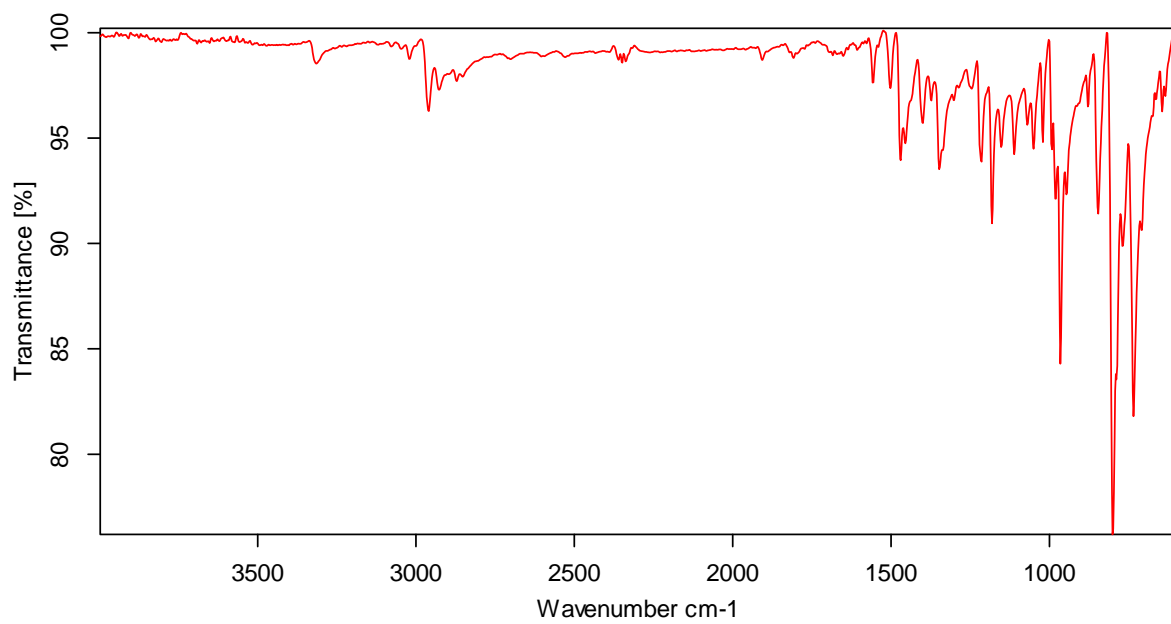


Figure S6. FTIR spectrum of (3, Ph-Sn).

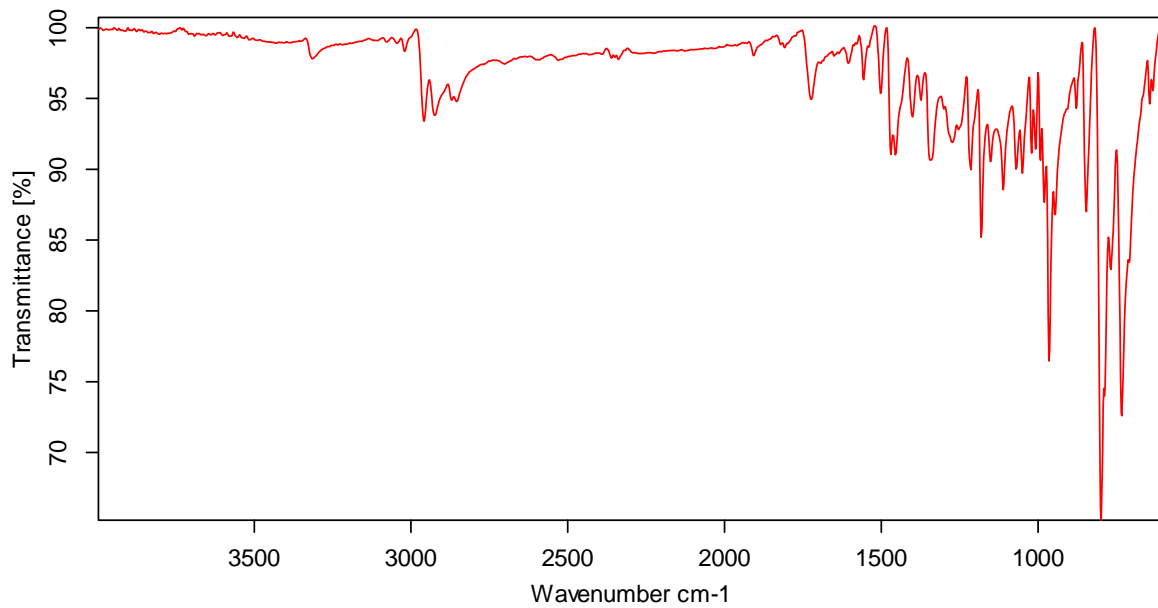


Figure S7. FTIR spectrum of (4, Ph-Mn).

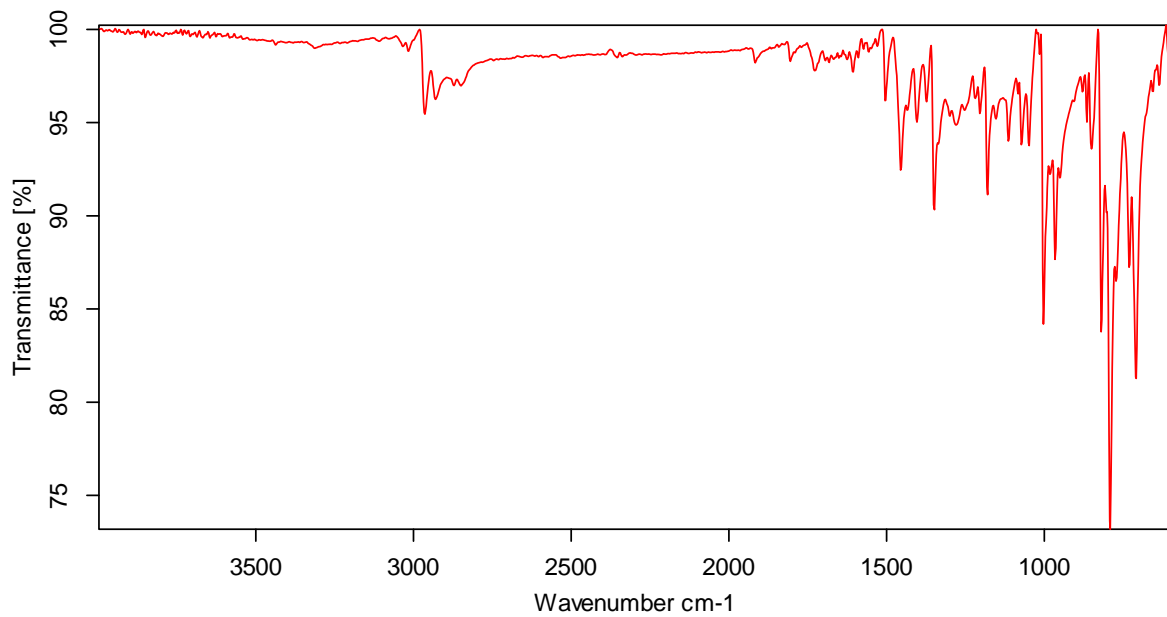


Figure S8. FTIR spectrum of (5, Ph-Ni).

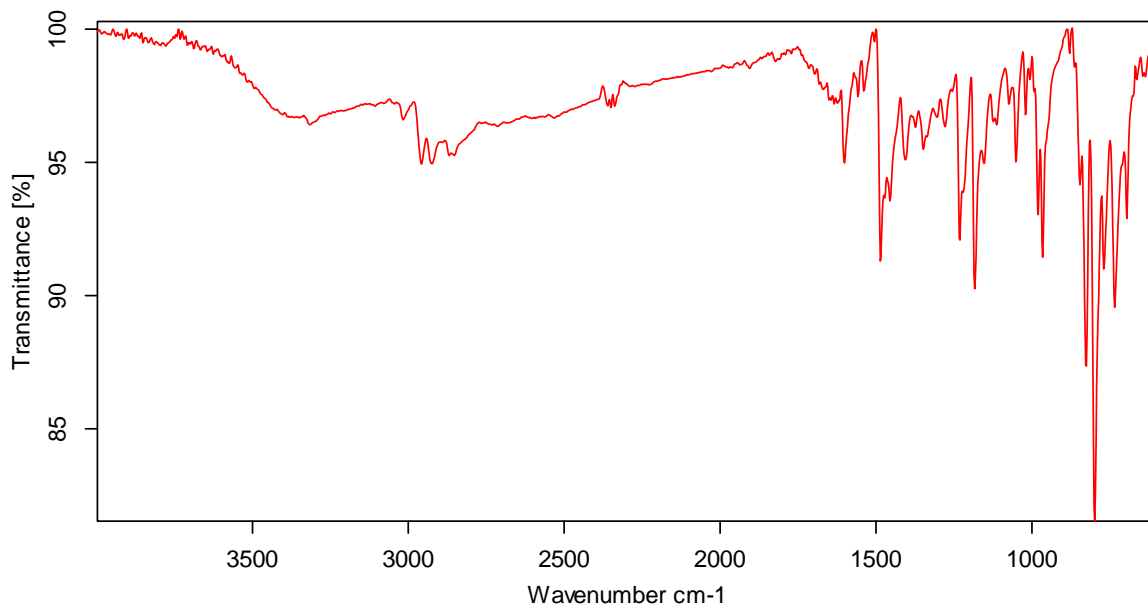


Figure S9. FTIR spectrum of (6, Ph-Al).

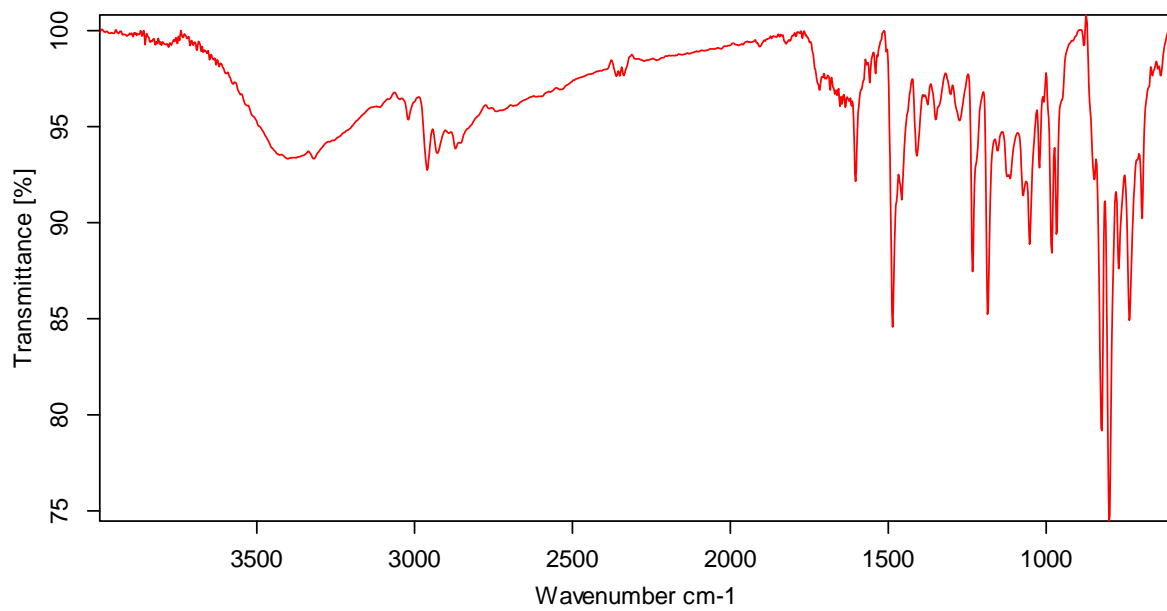


Figure S10. FTIR spectrum of (7, Ph-V).

UV- Vis spectra

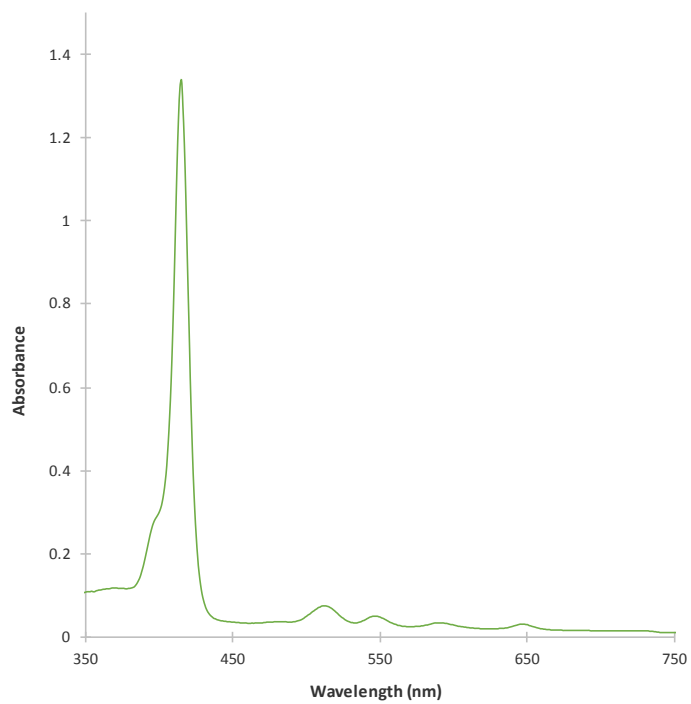


Figure S11. UV-Vis spectrum of (1, Ph) in ethyl acetate.

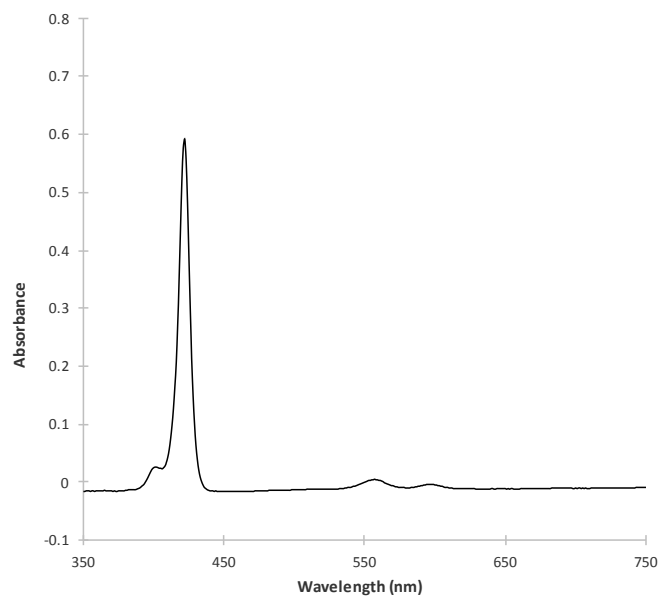


Figure S12. UV-Vis spectrum of (2, Ph-2) in ethyl acetate.

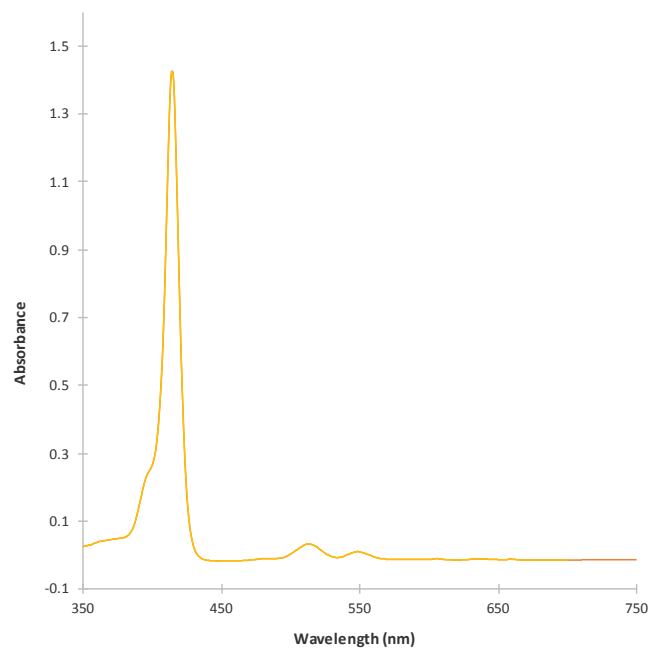


Figure S13. UV-Vis spectrum of (3, Ph-Sn) in ethyl acetate.

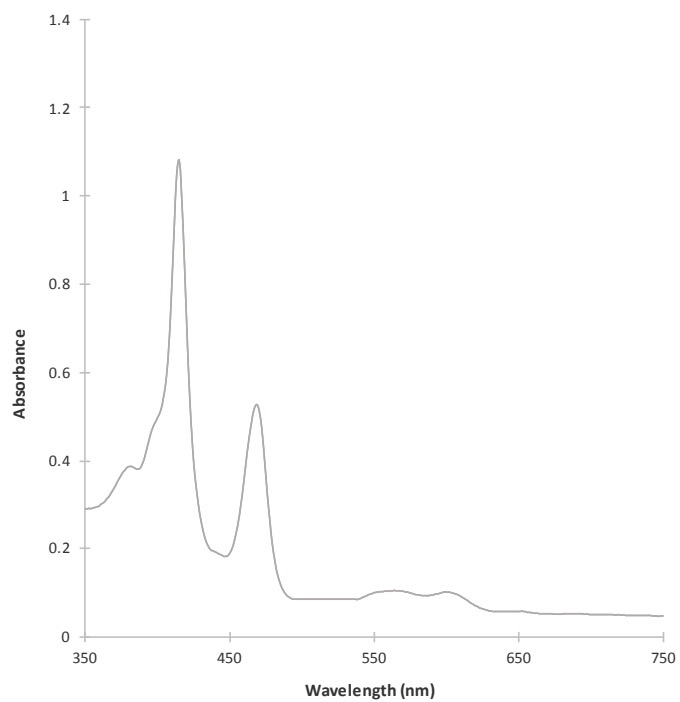


Figure S14. UV-Vis spectrum of (4, Ph-Mn) in ethyl acetate.

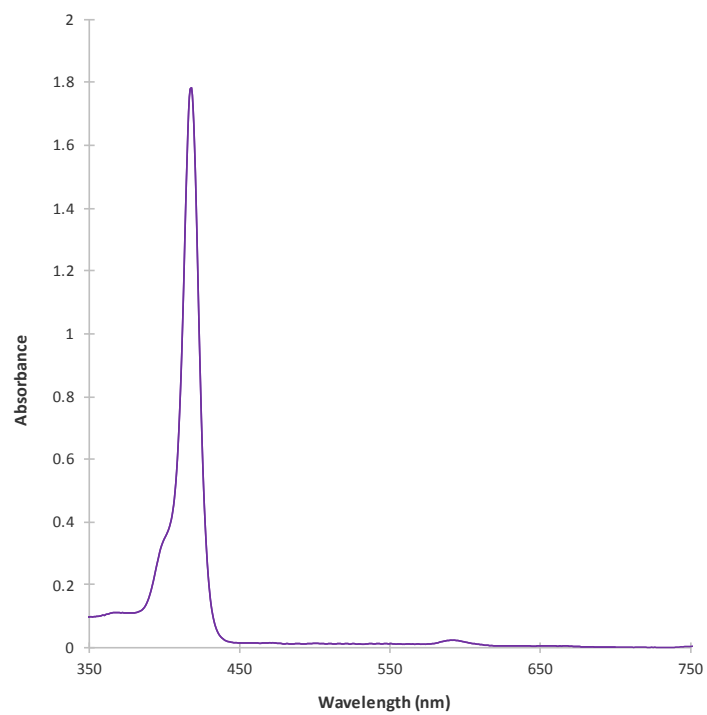


Figure S15. UV-Vis spectrum of (5, Ph-Ni) in ethyl acetate at room pH 7.0.

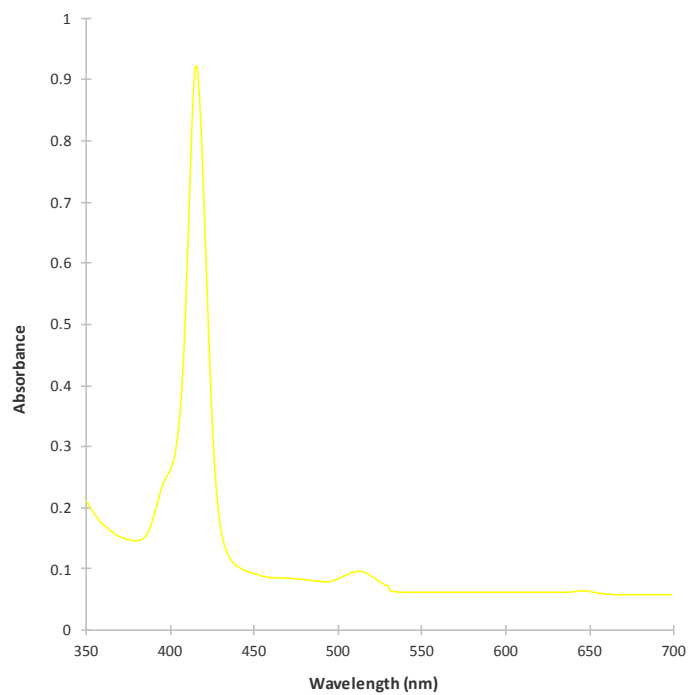


Figure S16. UV-Vis spectrum of (6, Ph-Al) in ethyl acetate.

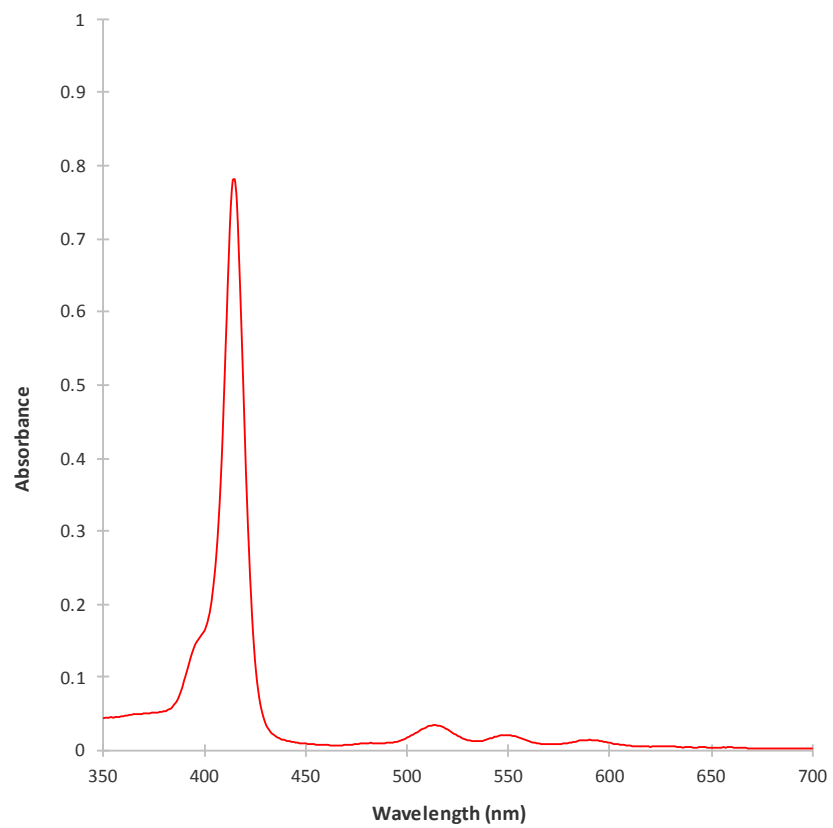


Figure S17. UV-Vis spectrum of (7, Ph-V) in ethyl acetate.

Fluorescence spectra

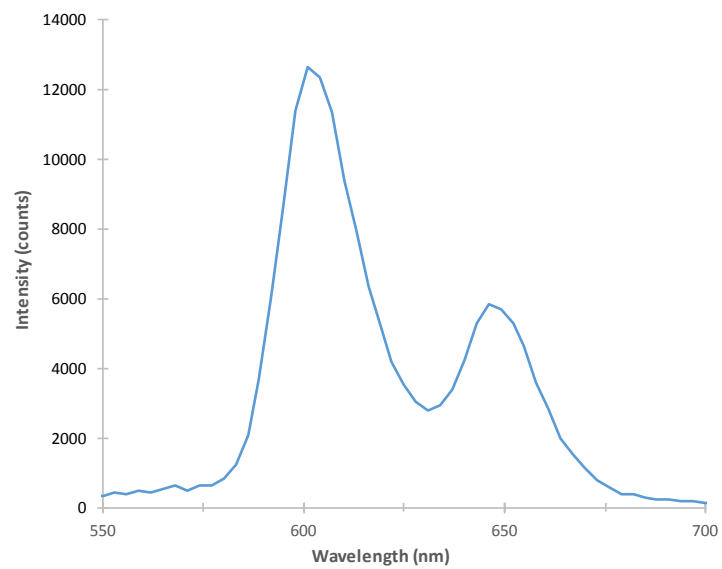


Figure S18. Emission spectrum of (1, Ph) in ethyl acetate.

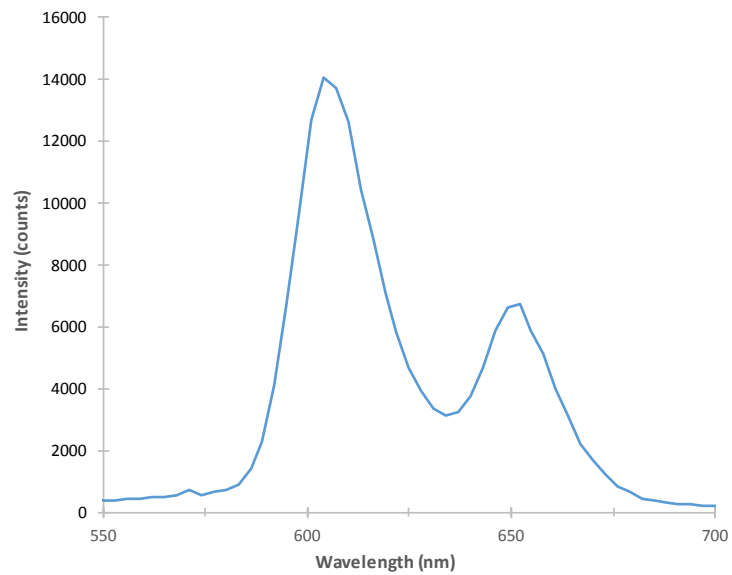


Figure S19. Emission spectrum of (2, Ph-Zn) in ethyl acetate.

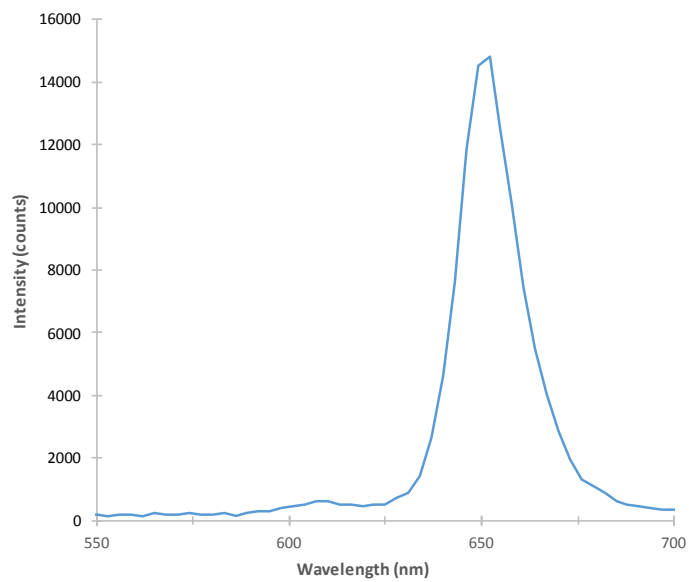


Figure S20. Emission spectrum of (3, Ph-Sn) in ethyl acetate.

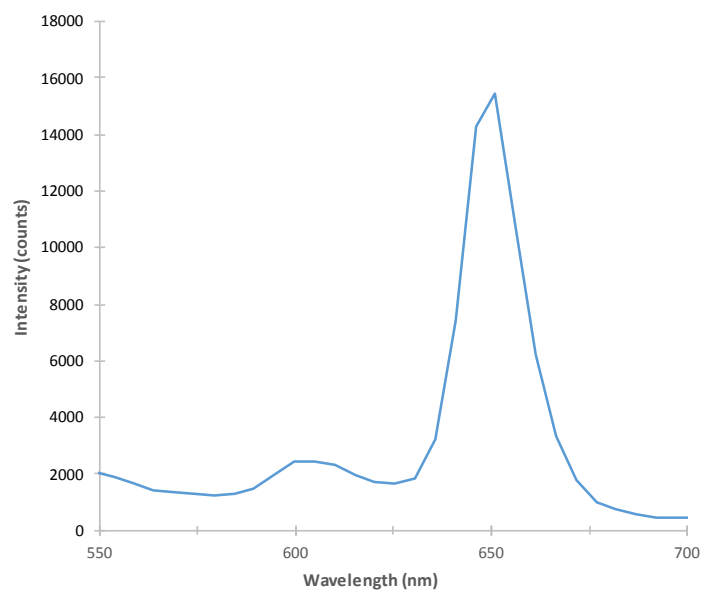


Figure S21. Emission spectrum of (4, Ph-Mn) in ethyl acetate.

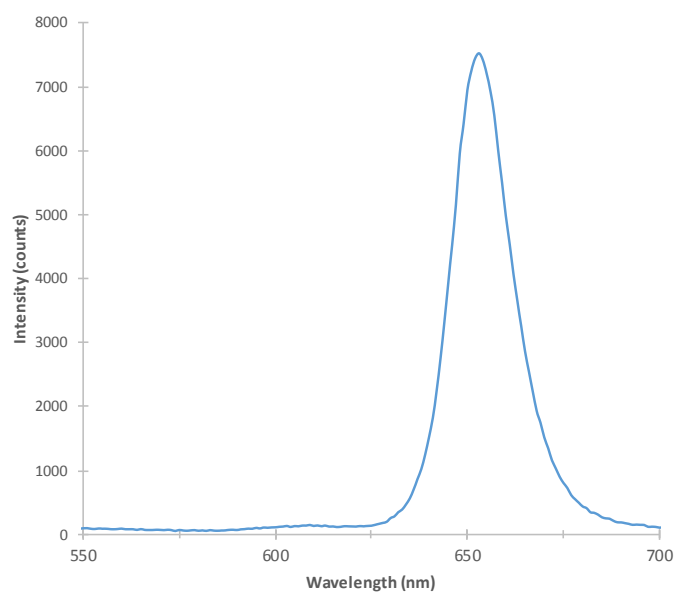


Figure S22. Emission spectrum of (5, Ph-Ni) in ethyl acetate.

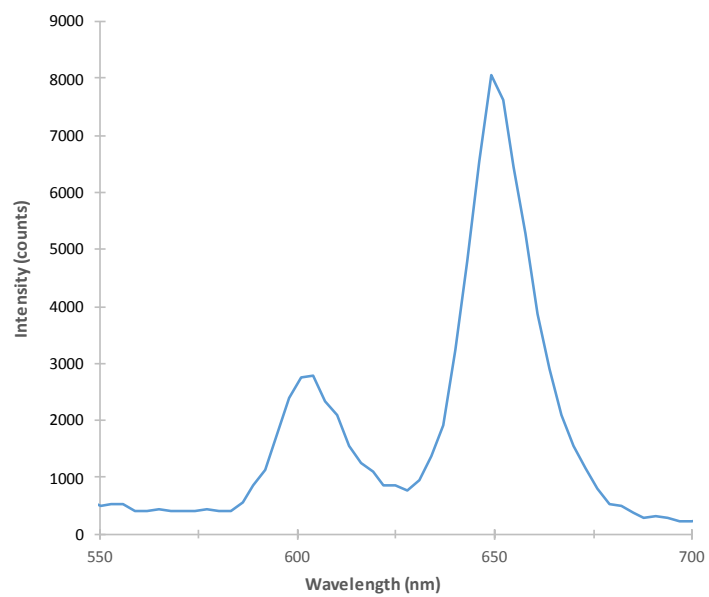


Figure S23. Emission spectrum of (6, Ph-Al) in ethyl acetate.

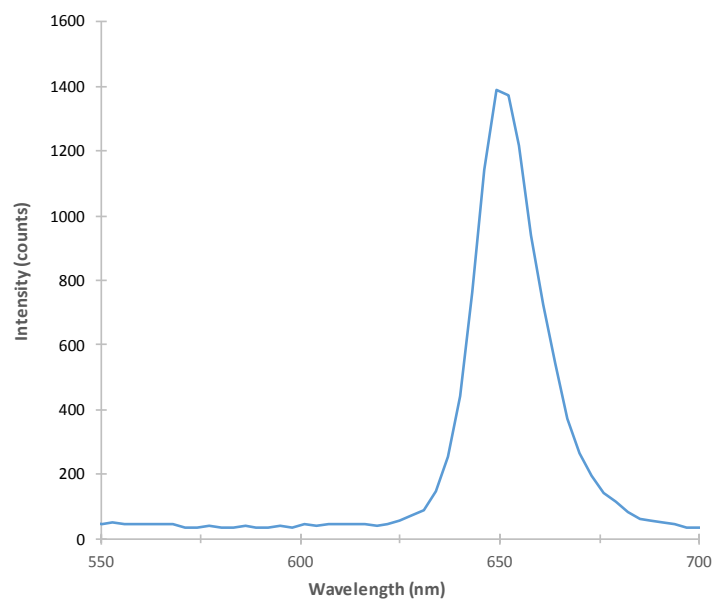


Figure S24. Emission spectrum of (7, Ph-V) in ethyl acetate.

Singlet oxygen plots

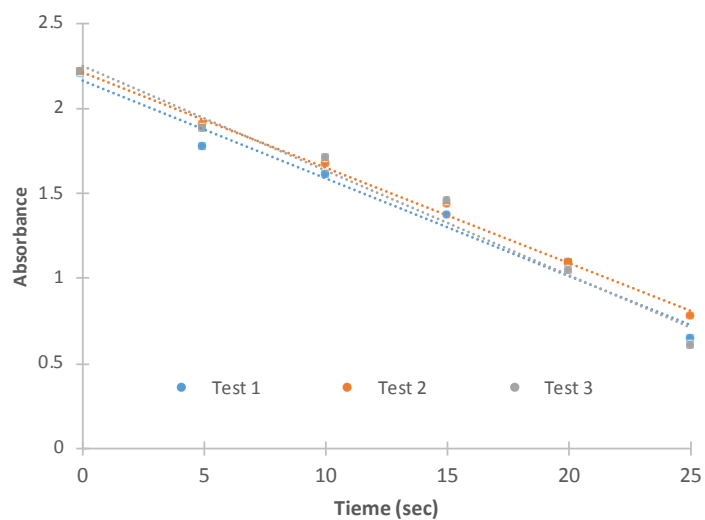


Figure S25. UV-Vis Absorbance of DPBF at 415 nm as a function of reaction time for (1, Ph), three tests are shown. Linear fitting is also shown.

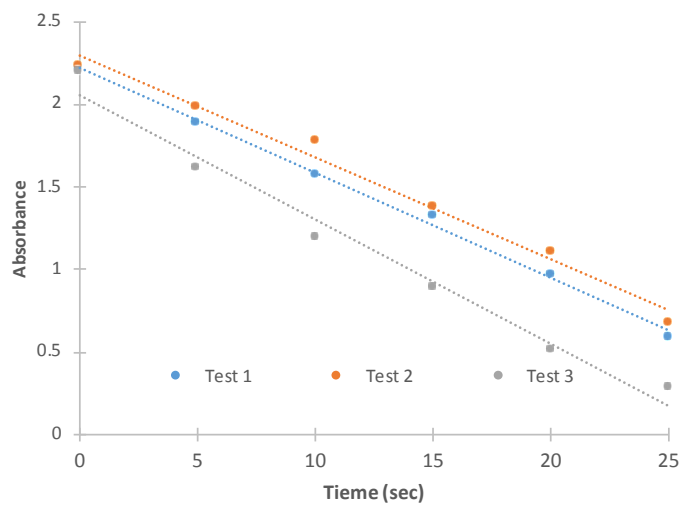


Figure S26. UV-Vis Absorbance of DPBF at 415 nm as a function of reaction time for (2, Ph-Zn), three tests are shown. Linear fitting is also shown.

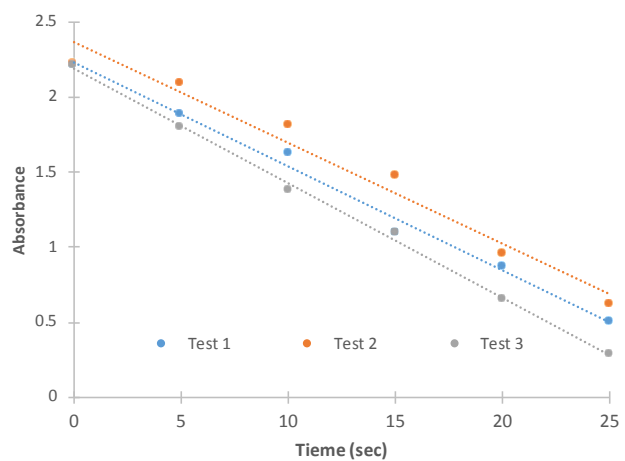


Figure S27. UV-Vis Absorbance of DPBF at 415 nm as a function of reaction time for (3, Ph-Sn), three tests are shown. Linear fitting is also shown.

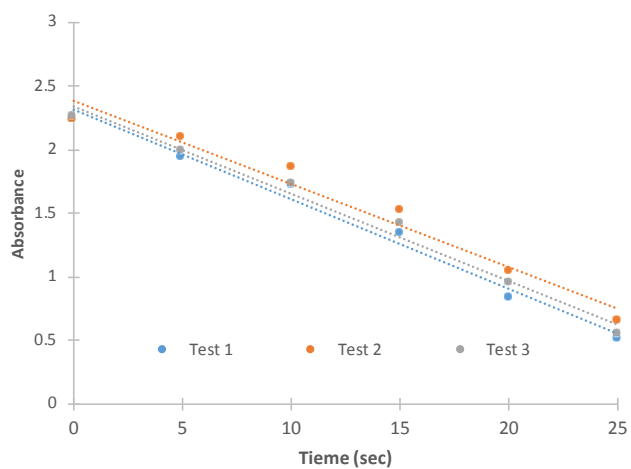


Figure S28. UV-Vis Absorbance of DPBF at 415 nm as a function of reaction time for (4, Ph-Mn), three tests are shown. Linear fitting is also shown.

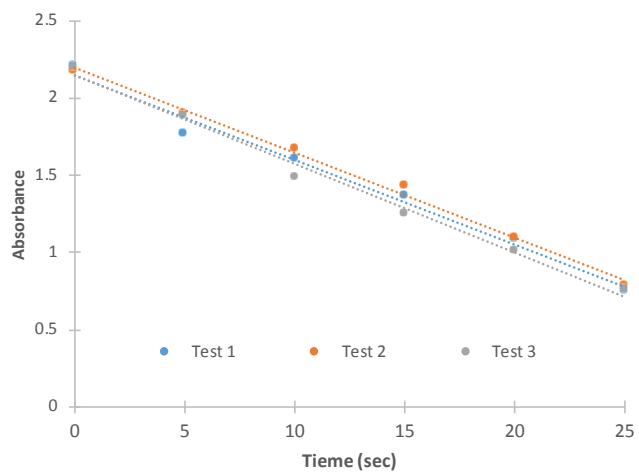


Figure S29. UV-Vis Absorbance of DPBF at 415 nm as a function of reaction time for (5, Ph-Ni), three tests are shown. Linear fitting is also shown.

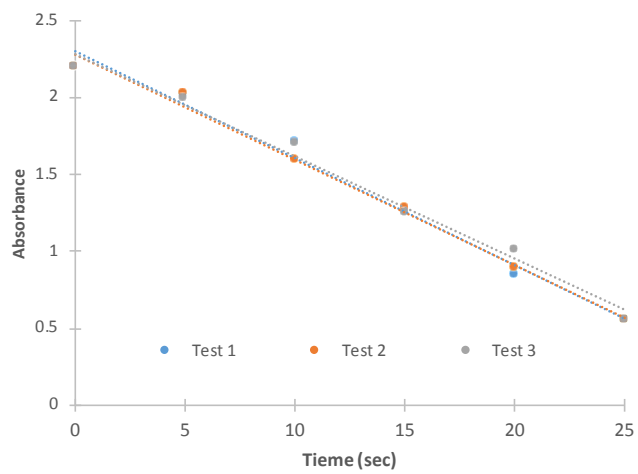


Figure S30. UV-Vis Absorbance of DPBF at 415 nm as a function of reaction time for (6, Ph-Al), three tests are shown. Linear fitting is also shown.

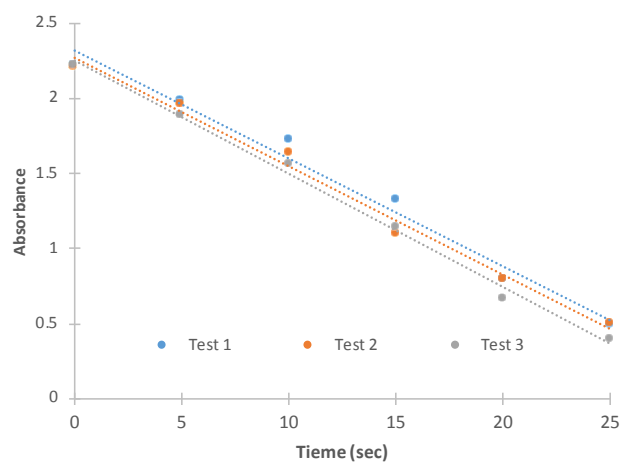


Figure S31. UV-Vis Absorbance of DPBF at 415 nm as a function of reaction time for (7, Ph-V), three tests are shown. Linear fitting is also shown.